

## Chemical Synthesis of Metal Nanoparticles in Aqueous Solutions with the Presence of Some Additives

(Sintesis Kimia Nanozarah Logam dalam Air dengan Kehadiran Beberapa Bahan Penambah)

MUNETAKA OYAMA\*, AKRAJAS ALI UMAR, MUHAMAD MAT SALLEH & BURHANUDDIN YEOP MAJLIS

### ABSTRACT

*Metal nanoparticles having interesting shapes can be prepared in aqueous solutions through simple reductions of metal ions with the presence of some additive reagents, such as cetyltrimethylammonium bromide and hexamethylenetetramine. In this review, some successful results for shape-controlled synthesis of metal nanoparticles in our group are summarized, which includes the synthesis of palladium nanocubes, palladium nanobricks, gold nanotripods. In addition, combining with indium tin oxide electrode surfaces, shape-controlled growth is shown to be possible to form gold nanoplates and copper oxide nanowires. Even in relatively mild synthetic conditions, interesting shape-controlled synthesis of metal nanoparticles is possible.*

*Keywords: Metal nanoparticle; nanobrick; nanocube; nanotripod*

### ABSTRAK

*Nanozarah logam dengan bentuk yang menarik dapat disediakan dalam larutan berair melalui proses penurunan sederhana ion logam dengan kehadiran beberapa bahan tambah reagen, seperti setiltrimetilamonium bromida dan heksametilentetramina. Dalam tinjauan ini, dikemukakan beberapa hasil sintesis nanozarah logam dengan bentuk terkawal yang berjaya disediakan oleh kumpulan kami, iaitu meliputi sintesis nanokubus dan nanobata paladium serta nanotripod emas. Di samping itu, dikemukakan usaha penumbuhan nanoplat emas dan nanowayar kuprum oksida di atas permukaan elektrod indium timah oksida. Meskipun hanya dengan menggunakan keadaan sintesis kimia yang sederhana, nanozarah logam dengan bentuk terkawal boleh disediakan.*

*Kata kunci: Nanobata; nanokubus; nanoplat; nanotripod; nanozarah logam*

### INTRODUCTION

Along with active interest to prepare metal nanoparticles (NPs) in recent years, a concept of shaped-controlled synthesis has become significant in the fields of nanoscience and nanotechnology. While spherical NPs might be dominantly formed without special controls, at present there are many examples where shape-controlled synthesis is possible to prepare metal NPs. For example, for the case of Au, Xia's group reported that the synthesis of Ag nanocubes, nanowires, nanospheres grown isotropically, nanoplates and nanobelts was possible with their hydrothermal method using ethylene glycol at 160°C by controlling the concentrations of the precursor, AgNO<sub>3</sub>, and poly(vinylpyrrolidone) (PVP) added in the solutions (Wiley et al. 2005). Tsuji's group successfully prepared Au nanostructures (spherical NPs, polygonal plates, nanorods and nanowires) and Ag nanostructures (spherical NPs, triangular nanoplates, nanorods, nanowires, nanosheets, nanotubes, and dendrites) by microwave-assisted synthesis (Tsuji et al. 2005).

In recent years, our group has been studying on the attachment of metal NPs on electrode surfaces (Oyama et al. 2010). By using chemical techniques, in particular, a seed-mediated growth method which was originally developed

for the synthesis of Au nanorods (Murphy et al. 2005), the attachment of NPs of Au (Kambayashi et al. 2005), Ag (Chang et al. 2005) and Pd (Chang et al. 2006b) on indium tin oxide (ITO) was found to be possible. In addition, PtNPs could be modified on ITO by a simple one-step reduction method (Chang et al. 2006a). While the electrochemical applications were summarized in our recent reviews (Oyama 2010; Oyama et al. 2010), it is interesting that some shape-controlled chemical synthesis of unique shaped NPs could be performed. As we have been utilizing the solution of cetyltrimethylammonium bromide (CTAB) in the growth process of the seed-mediated growth method, some additives can work for making featured structures even in aqueous solutions at room temperature.

In the present review, some successful results of shape-controlled synthesis of metal NPs in our group are summarized at first. The synthesis of palladium nanocubes, palladium nanobricks, gold nanotripods was possible in aqueous solutions. Next, combining with ITO electrode surfaces, shape-controlled growth was carried out to obtain gold nanoplates and copper oxide nanowires. These examples indicate that, even in relatively mild synthetic conditions, interesting shape-controlled synthesis of metal NPs is possible.

## SYNTHESIS OF MONODISPERSE PALLADIUM NANOCUBES

The preparation of nanocubes would be an interesting example in that the crystal-shape is manifested as the result of the delicate balance of three-dimensional crystal growth. El-Sayed and coworkers reported the formation of Pt nanocubes whose average diameter was ca. 11 nm using the reduction of  $\text{PtCl}_4^{2-}$  by  $\text{H}_2$  in the presence of polyacrylate (Ahmadi et al. 1996). Xia and coworkers reported the formation of Ag nanocubes, whose mean edge length was 80–115 nm (Sun & Xia 2002). For the Ag nanocubes, which could be used as the formation of nanoboxes having interesting optical properties (Chen et al. 2005), the large-scale synthetic method has been reported for monodisperse Ag nanocubes from 30 nm to 130 nm by the same group (Im et al. 2005). To prepare Ag nanocubes of ca. 55 nm, Yam and coworkers reported a CTAB modified silver mirror reaction, which permitted the controlled synthesis of monodisperse Ag nanocubes (Yu & Yam 2004).

Concerning the preparation of Pd nanocubes and cubooctahedrons, the Xia's group successfully utilized the polyol method (Xiong et al. 2005a; 2005c). In particular, they prepared Pd nanocubes of 8, 25, and 50 nm by using  $\text{FeCl}_3$  as an oxidative etchant for Pd seed particles (Xiong et al. 2005c). It seemed that 50 nm was a large edge length for Pd nanocubes, while it was 130 nm for Ag nanocubes (Im et al. 2005).

In our trial, the synthesis of Pd nanocubes whose edge length was ca. 85 nm was found to be possible (Chang et al. 2007). While the polyol method was used and the grown size was 50 nm (Xiong et al. 2005c), monodisperse Pd nanocubes of ca. 85 nm could be synthesized by simply reducing by ascorbic acid in the presence of CTAB and NaOH, i.e., using a manner similar to that of the Murphy's group for  $\text{Cu}_2\text{O}$  (Gou & Murphy 2003).

In the actual procedure, 0.5 mL of 0.01 M  $\text{K}_2\text{PdCl}_6$  aqueous solution was added into 18 mL of 0.1 M CTAB aqueous solution at 25°C. Then, 0.1 mL of 0.1 M ascorbic acid was added followed by the addition of 0.12 mL of 0.1 M NaOH, and the solution was left for 24 hours without stirring. After 24 hours the solution was centrifuged at 3500 rpm for 15 min to obtain black precipitate. The precipitate was then re-dispersed into pure water by sonication for 10

min, the suspension was dropped on the cleaned GC and dried in air for characterization.

Figure 1 shows the typical FE-SEM images of Pd nanocubes, which were synthesized by the above mentioned method, and then cast on the GC surface from the aqueous dispersion (Chang et al. 2007). It was clearly demonstrated that monodisperse Pd nanocubes whose edge length was ca. 85 nm was formed via the simple reduction by ascorbic acid in the presence of CTAB. Compared with the previous work (Xiong et al. 2005c), it was characteristic that larger Pd nanocubes of 85 nm formed at the room temperature.

As shown in Figure 1, the formation of 2D square array, not quasi-hexagonal array, was quite dominant even though the Pd nanocubes were simply cast on the smooth GC surface. The formation of the 2D square array is similar to the previous cases of Ag nanocubes (Sun & Xia 2002; Yu & Yam 2004). The present result seemed to be brought about by the presence of CTAB as the capping reagent. It is because the cohesive characteristics of CTAB had been reported for the case of  $\text{Cu}_2\text{O}$  nanocubes (Gou & Murphy 2003), and because the same CTAB adsorbed on Ag nanocubes has been reported to permit the formation of ordered 2D square array (Yu & Yam 2004).

The observation of UV-visible absorption for the solution of our 85-nm Pd nanocubes showed that the maximum of a broad absorption was 420 nm. This would be a reasonable red shift because the absorption has been reported at 330 nm for 25-nm Pd nanocubes and 390 nm for 50-nm Pd nanocubes (Xiong et al. 2005c).

Although the results in Figure 1 were obtained after synthesizing by the above mentioned procedures, the experimental conditions (e.g., the amount of the reagents) were those suitable for the formation of monodisperse 85-nm Pd nanocubes. For example, no cubic crystals but various irregular shaped crystals were obtained when CTAB is absent. When we use 0.05 M or 0.2 M CTAB solution instead of 0.1 M CTAB, smaller particles less than 20 nm were formed in solution. Thus, the concentration of CTAB was an important factor to form the nanocubes. The concentration of NaOH was also critical, for without the addition of NaOH, the formed nanocrystals were non-cubic.

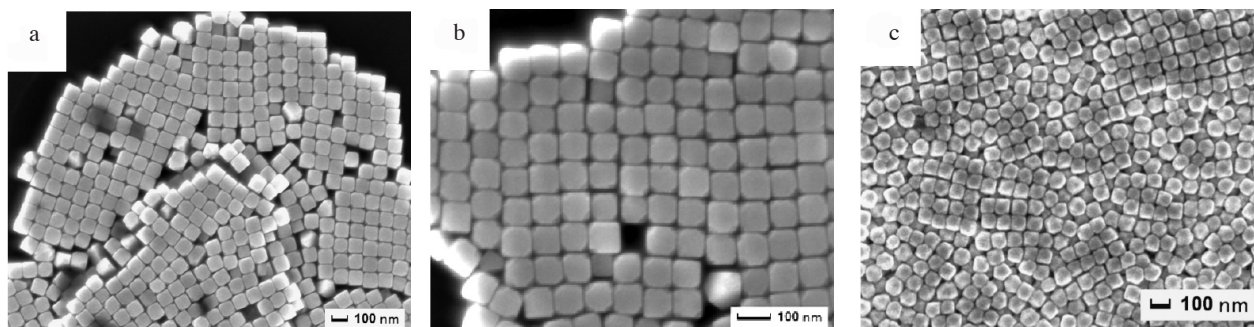


FIGURE 1. Typical FE-SEM images of Pd nanocubes prepared by the proposed method and assembled on the surface of glassy carbon. (a) (c) (c) show the images observed for the different parts and with different assemble methods. Reproduced from Chang et al. (2007), copyright 2007, with permission from Elsevier

The time course of the formed shape was followed by observing the FE-SEM images after 1, 4 and 12 hours. After 1 hour, the particle size grew up over 50 nm, but the shape was not cubic rather near spherical. After 4 hours, the shape approached to cubic accompanying the growth to 60 nm, but some irregularities were observed for the surfaces and edges. The FE-SEM image observed after 12 hours showed the formation of the similar Pd nanocubes, but the edges of the cubes were a little bit round. Thus, in the present case, it was considered that the formation or nucleation of Pd(0) to form nanoparticles were quick process during the period of the cube formation, and the cubic structures were formed gradually in the solution.

#### SYNTHESIS OF PALLADIUM NANOBLOCKS WITH ATOMIC-STEP DEFECTS

Using their polyol methods supported with an oxidative etching process, Xia's group produced Pd nanocubes (Xiong et al. 2005a) and triangular and hexagonal nanoplates (Xiong et al. 2005b), which was great success in view of the controlled synthetic growth of PdNPs that have very smooth surfaces in atomic level without the presence of any surface defects. However, many catalysis and adsorption processes of biomolecules on the NPs might occur on the surface defect sites, so that, the PdNPs that contain a large number of defect sites, such as atomic-steps, should be important in view of their practical applications.

We demonstrated that Pd nanobricks (NBS) that contain a large number of atomic-step defects on their surfaces could be easily prepared via the reduction of  $\text{PdCl}_6^{2-}$  using ascorbic acid in an aqueous mixture of CTAB and hexamethylenetetramine (hexamine, HMT) at room temperature (Ali Umar & Oyama 2008). By simply controlling the reaction parameters, such as the molar ratio,  $[\text{CTAB}]/[\text{HMT}]$  and the concentration of ascorbic acid, large-scale NBS structures could be obtained.

In the actual procedure, aqueous solutions of 0.01 M  $\text{K}_2\text{PdCl}_6$ , 0.01 M ascorbic acid, 0.1 M CTAB and 0.1 M HMT were prepared. For the formation of PdNBS, 5 mL of HMT was mixed with 15 mL of CTAB in a glass vial and agitated for several seconds. Thereafter, 0.5 mL of a dark-brown  $\text{K}_2\text{PdCl}_6$  solution was added to this solution. A bright yellowish-brown colored solution was then obtained. In the next step, 0.1 mL of 0.1 M NaOH was added and, then, properly agitated. Finally, 1 mL of an ascorbic acid solution was mixed with this solution followed by agitation for several seconds. The color of the solution immediately changed to copper-red after the addition of ascorbic acid, a reflection of the reduction of palladium ions. The reaction was then left undisturbed for 30 min at 28°C.

The precipitates of the PdNPs were obtained by centrifugation of the solution at 3000 rpm for 15 mins followed by multiple centrifugations in acetone (typically 3 times) and pure water. Eventually, the precipitate was re-dispersed in pure water. The dispersion in pure water was stable for several days if store in a refrigerator. For the

FE-SEM and HRTEM analyses, the NPs dispersion in ethanol was used.

Figure 2(a) and (b) show typical FE-SEM images of the PdNBS prepared using the present approach. Large-scale NBS structures (> 70% of the product) could be successfully prepared (Ali Umar & Oyama 2008). The powder X-ray diffraction experiment performed on the as-prepared samples confirmed that these NPs are pure Pd without the presence of any impurity as well as oxide formation. These new structures self-assembled side-by-side of each other during the solvent drying forming a 3-dimensional superstructure. This could be directly related to the result of minimizing the high-surface energy possessed by such fcc metal nanocrystals due to the presence of CTAB. The PdNBS exhibit a gradient in their short-axis which ranges from 20 to 60 nm forming a slanted topology along its long-axis. The lengths of the PdNBS were found to be in the range of 80 to 500 nm. High-resolution FE-SEM observations on the surface as well as on the slanted region of the PdNBS (Figure 2(d)-(e)) revealed the formation of a type of atomic-step or kink structure, a characteristic which may make them potential as catalyst for multiple specific reactions with the target molecules.

The details of the structure and the surface morphology of the as-prepared PdNBS were investigated using the HRTEM technique (Figure 3). Although the NBS surface contains a large number of stepped structures, based on the FE-SEM images, the HRTEM results surprisingly revealed that the bulk PdNBS are single crystalline in nature, which is indicated by the presence of a regular lattice fringe without any twinning or stacking-fault. From the image, it was found that the lattice fringe spacing is ca.  $\sim 2 \text{ \AA}$  which belongs to the  $\{100\}$  crystal plane of the fcc Pd nanocrystal. From the HRTEM characterization on the surface that contains a stepped or defect structure (Figure 3(c)-(d)), it was found that the PdNBS are comprised of a several-atom thick step on the surface that is sketched on the image. No twinning or stacking faults as well as bulk-nano-interfacing formation exist for these kinds of defects, further confirming that the PdNBS have a single crystalline characteristic.

The procedure for the formation of the PdNBS structure presented here is very simple and quick with an aqueous phase synthetic process. In a typical procedure, the Pd nucleation occurred within seconds after the addition of the ascorbic acid to the reaction. It is indicated by the change in color of the solution from a light-brown ( $\text{K}_2\text{PdCl}_6$ ) to a copper-red, a reflection of the reduction of  $\text{Pd}^{\text{IV}}$  to  $\text{Pd}^0$ . The color of the solution remained stable until ca. 3 minutes and then gradually changed to light-grey in the final process. The UV-vis absorption spectra recorded during the growth process indicated the presence of three surface plasmon resonance (SPR) bands of the PdNPs centered at 373, 448 and 532 nm during the initial reaction process confirming the formation of NPs. These bands gradually broaden with time and finally leave a single broad band centered at 423 nm at the end of the reaction (after 30 min.) inferring the formation of a bigger PdNBS structure.

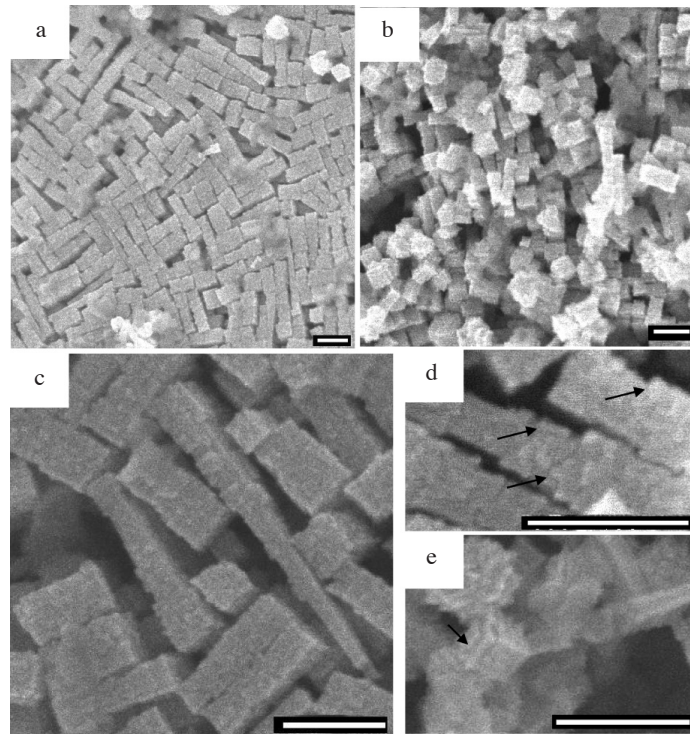


FIGURE 2. FE-SEM image of PdNBs prepared using the present method. (a) FE-SEM images of three-dimensional superstructure assembly of bigger PdNBs structures. (b) FE-SEM images of smaller nanobrick and nanocube byproducts. (c-e) High-resolution FE-SEM images of bigger PdNBs showing atomic-step surfaces. The PdNPs were prepared using a 20 mL growth solution that contains 0.25 M of  $K_2PdCl_6$ , 75 mM of CTAB, 25 mM of HMT, 1 mM of NaOH and 0.50 mM of ascorbic acid. Scale bar is 100 nm. Reproduced from Ali Umar & Oyama (2008), copyright 2008, with permission from the American Chemical Society

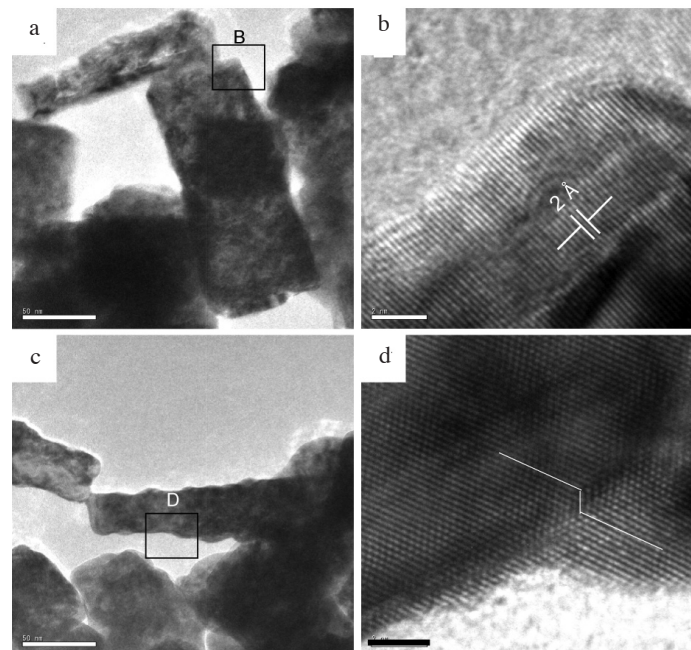


FIGURE 3. (a-c) Typical TEM image of PdNBs. (b) High-resolution TEM (HRTEM) image of PdNBs indicates an ordered lattice fringe pattern without the presence of twinning or stacking fault with spacing of  $\sim 2 \text{ \AA}$ , which is attributed to the  $\{001\}$  crystal plane. (d) HRTEM image of PdNBs showing atomic-steps (sketched for clarity). Scale bar are 50 nm (a and c) and 2 nm (b and d). Reproduced from Ali Umar & Oyama (2008), copyright 2008, with permission from the American Chemical Society

In order to produce a high yield of PdNBs structures, the concentration ratio between CTAB and HMT in the reaction should be 3:1. If the ratio is lower or higher than this value, no PdNBs structures were formed, but instead nanocubes. A slight modification of the ratio of CTAB and HMT from the optimum value causes a drastic change in the entire structural growth of the PdNPs, further confirming the importance of such a parameter for the formation of the PdNBs structures.

In addition, the concentration of ascorbic acid in the reaction should be around 0.50 mM in order to have enough power to accelerate the reduction of  $K_2PdCl_6$ . A lower ascorbic acid concentration may cause a decrease in the reduction rate of the Pd-salts which leads to the formation of a dominant, larger-size nanocube product. However, if the relatively high ascorbic acid concentration was used, no PdNBs were formed, but instead truncated-nanocubes with a high surface defect. This could be as the result of attachment of the excess ascorbic acid onto the nanocrystal surfaces of which in turn inhibit the elongation of the nanocube structure and then induce the formation of defect structures on the nanocube surface. Furthermore, the NaOH concentration should be relatively low, typically ca. ~1 mM.

This result would be an interesting example that the new structures of PdNBs with a large number of atomic-step defects could be easily prepared in aqueous solutions at room temperature. The formed PdNBs might have potentials for catalytic, electronics and optoelectronics applications.

#### HIGH-YIELD SYNTHESIS OF TETRAHEDRAL-LIKE Au NANOTRIPODS

Since NPs' properties strongly depend on their shape, novel properties and more enhanced functions could be further obtained if such NPs are prepared in the form of high-order shape-anisotropy, such as tripod and tetrapod topology. However, concerning noble metals, the reports of the formation of tripod or tetrapod are not many. As for Au nanotripods and tetrapods, Chen et al. reported the method using  $HAuCl_4$ , CTAB, concentrated silver and NaOH (Chen et al. 2003). In their work, the clear atomic orders in Au tripod nanocrystals were shown using TEM; however, the yield of Au tripods was reported as ~9% together with the formation of mono-, bi- and tetra-pods, but with the dominant sphere formation (~40%). Synthesis and optical properties of "branched" Au nanocrystals were reported by Hao et al. (2004); using bis-(p-sulfonatophenyl)-phenylphosphine dehydrate dipotassium and  $H_2O_2$ , branched Au nanocrystals with one, two or three tips were synthesized in over 90% yield (the majority, three-tipped NPs, was over 50%). It is noticeable that the shape-dependent red-shift (by 130-180 nm from nanospheres) of branched Au nanocrystals has been shown with the successful simulations for the Au nanocrystal with three-tips. Later, Huang and coworkers reported the formation of branched Au nanocrystals by a seeding growth and a

direct method (Kuo & Huang 2005; Wu et al. 2006). While the shapes of nanocrystals were slightly different from the previously reported ones (Chen et al. 2003; Hao et al. 2004), interesting transformation processes of the branched Au nanocrystals were reported.

We proposed a new strategy for synthesizing Au nanotripods with high-yield (Ali Umar & Oyama 2009). By simply using an aqueous solution of binary mixture of CTAB and HMT as a media for the reduction of  $AuCl_4^-$ , a facile but effective synthesis of Au nanotripods was possible at room temperature after manipulating the reagent concentrations.

As a typical procedure, 25 mL solution that contains 1.0 mL of 0.01 M  $HAuCl_4$ , 5 mL of 0.1 M CTAB, 5 mL of 0.1 M HMT and 15 mL pure water was prepared. The color of the solution was bright brown-yellowish at this stage. After that, 0.5 mL of 0.01 M ascorbic acid was added, and the solution immediately changed to colorless, indicating the reduction of Au(III) to Au(I). Finally, 100  $\mu$ L of 1 M NaOH was added to the reaction. Under these conditions, the final solution contains 0.4 mM, 20 mM, 20 mM, 0.2 mM and 4 mM of  $HAuCl_4$ , CTAB, HMT, ascorbic acid and NaOH, respectively. The color of the solution changed from colorless to blue within seconds after the addition of NaOH indicating the formation of AuNPs. The solution was left undisturbed for 5 min and, then, centrifuged at 3000 rpm for 15 min. A blue precipitate is then collected and dispersed in water. For the FE-SEM and HRTEM characterization, Au nanotripods dispersion in ethanol was used. The NPs dispersion both in water or ethanol can be stable for one day if sealed and stored in a refrigerator. All the reaction was performed at room-temperature, ca. 25°C.

Figure 4(a) shows the FE-SEM image of AuNPs, which were prepared and separated as described above. In the optimal conditions, characteristic shaped Au nanotripods were obtained with yield as high as ~80% of the product. The Au nanotripods were found to self-assemble and form a 3D-superstructure upon solvent drying as shown in Figure 4(a). The present nanotripods featured three-arms (diameter ~ 10 nm) projecting from a core-like structure of which are equal in length (ca. ~ 20-50 nm) to within a few percent. Interestingly, these arms did not grow in-plane to each other, but adopted a tetrahedral-like symmetry (inset Figure 4(b)) with Y-shape topology instead of high-symmetry tripod structure. This result is in contrast to those obtained using the previous methods, by which in-plane pods growth has been reported (Chen et al. 2003; Hao et al. 2004; Kuo & Huang 2005; Wu et al. 2006). Others byproducts, such as tear-drop, bipod, tetrapod, fusiform (~10%) and irregular-shape (~10%) particles were also obtained.

Figure 4(b) shows low-resolution TEM image of single Au nanotripod. Higher contrast at the core region compare to the arms is recognized from the image inferring they are at a difference level from the grid plane - the three arm-tips touch the plane while the core elevate to a certain

distance, the result further confirming the geometry of tripod, namely tetrahedral-like structure. Figures 4(c) and (d) give the HRTEM image at the core-arm interface and at the arm of tripod as indicated with white squares in Figure 4(b). At the core-arm interface region, no indication of lattice twinning was observed. These fringes continuously extended throughout the NPs reflecting the tripod has a single crystalline characteristic. Our observation on one arm of the tripod measured a lattice fringe spacing of 0.239 nm, which is belong to the  $\{111\}$  planes (Figure 4(d)). Taking into account of the NPs' geometry, it can be concluded that the nanotripod in fact have a core structure with a (111) basal plane that lie parallel to the surface and three-arms projecting toward  $[010]$ ,  $[00-1]$  and  $[-1-10]$  directions.

The formed nanoshapes were very sensitive to the concentrations and the ratio of CTAB and HMT. To produce the tetrahedral-like Au nanotripods with high yield, the optimum ratio between CTAB and HMT was 1:1. If the concentration of CTAB is higher than that of HMT, less symmetry tripods were formed; if the concentration of CTAB is lower, low-aspect ratio tripod nanocrystals were formed. HMT indicated a crucial function in the formation of branched-topology. This implies that HMT capped or adhered on specific surfaces selectively to form the pod-

like structure. Another important controlling factor for fine-tuning the shape of Au nanotripods was the ratio between  $\text{HAuCl}_4$  and the sum of the concentrations of CTAB and HMT. As the results of increasing the sum of the concentrations from 24 mM to 64 mM, with keeping the CTAB/HMT ratio as unity and the  $\text{HAuCl}_4$  concentration as 0.4 mM, it was found that the arm-length and -diameter of the nanotripods increased.

Along with the changes in nanoscopic size of tripods, we could observe systematic changes in plasmonic absorption (Ali Umar & Oyama 2009). Reflecting the high-yield of the proposed method, a single peak at 670 - 800 nm was dominant in each spectrum, which is similar to the previous result (Hao et al. 2004). Thus, the longitudinal surface plasmon band (L-SPR) at longer wavelength is considered to have appeared mainly for Au nanotripods, while small peaks of the transversal surface plasmon band (T-SPR) were recognized around 520 nm. It is evident that Au nanotripods have unique plasmon peaks that are different from those of Au nanorods, and further that the wavelengths are sensitive to the nanosize of formed tripods.

As the effects of the concentrations of  $\text{HAuCl}_4$ , it was also found that 0.4 mM was optimal to form Au nanotripods. When the concentration was increased,

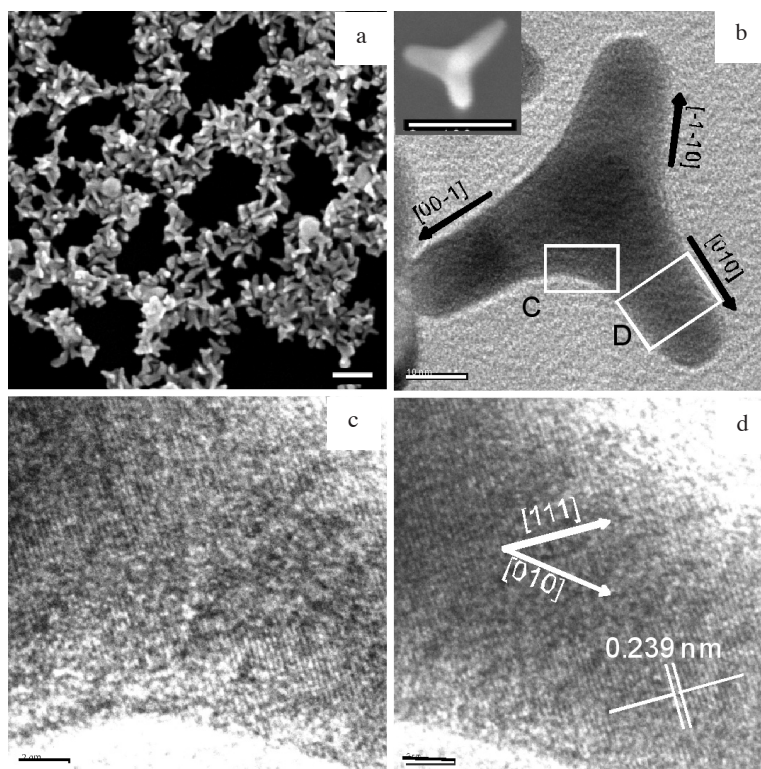


FIGURE 4. (a) FE-SEM image of Au nanotripods prepared in the standard solution, i.e., 1.0 mL of 0.01 M  $\text{HAuCl}_4$  in 25 mL of CTAB (20 mM) and HMT (20 mM) mixture, 0.5 mL of 0.01 M ascorbic acid and 0.1 mL of 1 M NaOH. (b) Low-resolution TEM image of single nanotripods. Inset shows a truncated-tetrahedral-like geometry of tripod. (c-d) High-resolution TEM image of arm-core interface and arm structure of nanotripods. Scale bar: (a) 100 nm, (b) 10 nm, (c-d) 2 nm and inset 100 nm. Reproduced from Ali Umar & Oyama (2009), copyright 2009, with permission from the American Chemical Society

the formed NPs became fatter and bigger, and no more nanotriplets at 0.8 mM. On the other hand, while the optimum NaOH concentration for high-yield nanotriplets growth was 4 mM, big nanotriplets and dominant quasi-spherical NPs were obtained at 2 mM. At higher NaOH concentration at 12 mM, the formed nanotriplets became so unstable that we could not obtain Au nanotriplets after the centrifugal treatment. Thus, it was expected that the Au nanotriplets formed with 12 mM NaOH are unstable and quickly transformed into a more stable geometry due to an active Oswald roughening process.

As for the formation mechanism, the presence of HMT is considered to be a key factor to allow the structural growth. By mixing together with CTAB, which form anisotropic micelles structures (such as rod and wire) over 20 mM (Törnblom & Henriksson 1997), it is considered that the interesting tetrahedral-like Au triplots could be formed with HMT. To mix CTAB and HMT are also important since another micelle structure might be formed as in the case of CTAB with others chemicals (Lin et al. 1994).

#### FORMATION OF Au NANOPlates AND CuO NANOWIRES ON ITO

Until the previous section, the NPs were prepared in aqueous solutions and corrected for evaluations. However, some shape-controlled NPs would be formed on substrates using a similar wet-chemical approach in aqueous solutions at room temperature. Here, we would like to show two successful results of the formation of nanostructures on the surface of ITO.

As the first example, to attach Au nanoplates on ITO surfaces, we permitted the two-dimensional crystal growth of Au through the liquid phase reduction from Au nano-seed particles attached on the ITO surface using poly(vinylpyrrolidone) (PVP) instead of CTAB as a capping reagent in the growth solution (Ali Umar & Oyama 2006). By controlling the concentration of PVP, the formation of Au nanoplates was possible as shown in Figure 5(a). The surface coverage with Au nanoplates was as high

as roughly 30%, though various shaped Au nanocrystals were concurrently formed on the ITO surface. The Au nanoplates were single crystalline in nature with (111) basal planes, and the edge-length was up to ca.  $\sim 2 \mu\text{m}$ , growing parallel to the ITO surface. The concentration of PVP in the growth solution was a key factor for the formation of Au nanoplates, because spherical or irregular shaped AuNPs were formed at higher or lower concentrations of PVP. The absorption spectra of Au nanoplate-attached ITO implied anisotropic and specific optical characteristics of the modified ITO glasses.

To improve the coverage and attachment of Au nanoplates on ITO, we proposed a revised method using the binary surfactant mixture of PVP and CTAB (Ali Umar et al. 2009). The formation of Au nanoplates strongly depended on the concentration of PVP, while the nanoplate size depended on the CTAB concentration. In typical process with optimum PVP and CTAB concentrations, 60% of the nanocrystal product was nanoplates as shown in Figure 5(b). Triangular nanoplates were found to be the major shape of the nanoplates with yield up to ca. 50%, while the hexagonal or truncated-hexagonal and rounded-nanoplates shared up to ca. 30 and 20% of the nanoplates products, respectively. The nanoplates were characterized by a very thin structure with thickness less than 10 nm. The edge-length size of the nanoplates was found to be up to ca. 1  $\mu\text{m}$ . At an optimum growth condition, ca. 70% of the surface area was covered by nanoplates. X-ray diffraction result on the surface modified nanoplates samples indicated an exceedingly high Au(111) peaks of Au nanocrystal without the presence of other peaks, such as (200) and (220), in the diffraction spectrum.

In addition, most recently we reported a simple approach to grow highly thin and electron transparent Au nanoplates with a micrometer range edge-length dimensions (Ali Umar et al. 2010). The thin nanoplates were obtained by realizing an effective two-dimensional crystal growth of the nanoseed in a ternary surfactant mixture of CTAB, PVP and poly(ethylene glycol).

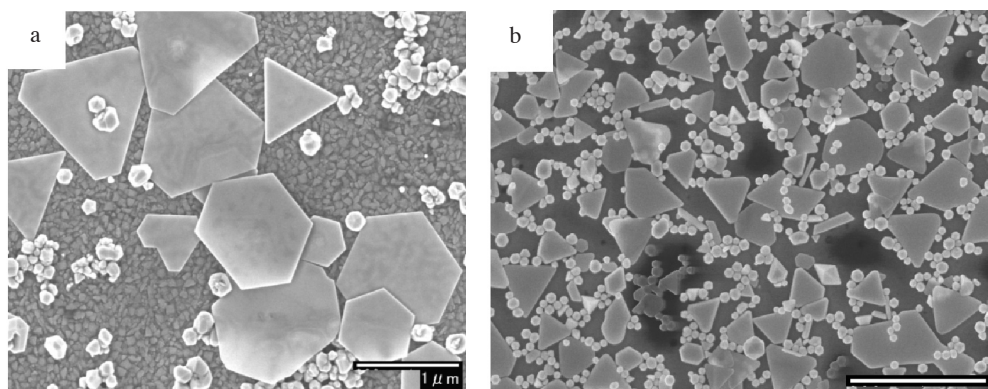


FIGURE 5. FE-SEM images of Au nanoplates attached and grown on ITO surfaces prepared by the methods (a) in Ali Umar & Oyama (2006) and (b) in Ali Umar et al. (2009). Reproduced from Ali Umar & Oyama (2006) and Ali Umar et al. (2009), copyright 2006 and 2009, with permission from the American Chemical Society

On the other hand, a large scale vertical array of single-crystalline CuO nanowires could be prepared on ITO surfaces using the seed-mediated growth method (Ali Umar & Oyama 2007). The procedure simply involved a room-temperatures liquid–solid growth process of attached CuO nanoseeds on ITO surface in the mixed aqueous solution of  $\text{Cu}(\text{CH}_3\text{COO})_2$  and  $\text{NH}_3$ . By controlling the concentration of the chemical precursors in the growth solution, we can fabricate variable-shape 1D structures of CuO, such as nanowires and nanobelts. The FE-SEM image analysis indicated that these nanowires feature uniform size with tiny structures that have diameters and lengths in the range of 10 and 100 nm, respectively, and tend to form a bundlelike structure at the top end of the wires. The XRD analysis of the samples revealed that the nanostructures were a high-crystalline CuO without the presence of other phases of the Cu complexes.

### CONCLUSIONS

In this review, we summarized successful results of shape-controlled chemical synthesis of metal NPs. The shape-controlled synthesis of NPs is interesting from the view of fundamental nanoscience for mechanistic elucidation of the bottom-up nanostructuring. In addition, interesting shaped NPs should have potentials in certain applications of nanotechnology. As the next stage, making efforts to find applicability of interesting shaped NPs are desirable as well as the varieties of nanostructure making.

The nanostructuring may have an impression that there are some difficulties in techniques and costs. However, we would like to emphasize that interesting shape-controlled synthesis of metal NPs would be possible in relatively mild synthetic conditions, e.g., at room temperature and in aqueous solutions, as elaborated in this review.

### REFERENCES

- Ahmadi, T.S., Wang, Z.L., Green, T.C., Henglein, A. & El-Sayed, M.A. 1996. Shape-Controlled Synthesis of Colloidal Platinum Nanoparticles. *Science* 272: 1924-1925.
- Ali Umar, A. & Oyama, M. 2006. Formation of Gold Nanoplates on Indium Tin Oxide Surface: Two-Dimensional Crystal Growth from Gold Nanoseed Particles in the Presence of Poly(vinylpyrrolidone). *Crystal Growth & Design* 6(4): 818-821.
- Ali Umar, A. & Oyama, M. 2007. A Seed-Mediated Growth Method for Vertical Array of Single-Crystalline CuO Nanowires on Surfaces. *Crystal Growth & Design* 7(12): 2404-2409.
- Ali Umar, A. & Oyama, M. 2008. Synthesis of Palladium Nanobricks with Atomic-Step Defects. *Crystal Growth & Design* 8(6): 1808-1811.
- Ali Umar, A. & Oyama, M. 2009. High-Yield Synthesis of Tetrahedral-Like Gold Nanotripods Using an Aqueous Binary Mixture of Cetyltrimethylammonium Bromide and Hexamethylenetetramine. *Crystal Growth & Design* 9(2): 1146-1152.
- Ali Umar, A., Oyama, M., Mat Salleh, M. & Yeop Majlis, B. 2009. Formation of High-Yield Gold Nanoplates on the Surface: Effective Two-Dimensional Crystal Growth of Nanoseed in the Presence of Poly(vinylpyrrolidone) and Cetyltrimethylammonium Bromide. *Crystal Growth & Design* 9(6): 2835-2840.
- Ali Umar, A., Oyama, M., Mat Salleh, M. & Yeop Majlis, B. 2010. Formation of Highly Thin, Electron-Transparent Gold Nanoplates from Nanoseeds in Ternary Mixtures of Cetyltrimethylammonium Bromide, Poly(vinyl pyrrolidone), and Poly(ethylene glycol). *Crystal Growth & Design* 10(8): 3694-3698.
- Chang, G., Oyama, M. & Hirao, K. 2006a. In Situ Chemical Reductive Growth of Platinum Nanoparticles on Indium Tin Oxide Surfaces and Their Electrochemical Applications. *The Journal of Physical Chemistry B* 110(4): 1860-1865.
- Chang, G., Oyama, M. & Hirao, K. 2006b. Seed-Mediated Growth of Palladium Nanocrystals on Indium Tin Oxide Surfaces and Their Applicability as Modified Electrodes. *The Journal of Physical Chemistry B* 110(41): 20362-20368.
- Chang, G., Oyama, M. & Hirao, K. 2007. Facile synthesis of monodisperse palladium nanocubes and the characteristics of self-assembly. *Acta Materialia* 55(10): 3453-3456.
- Chang, G., Zhang, J., Oyama, M. & Hirao, K. 2005. Silver-Nanoparticle-Attached Indium Tin Oxide Surfaces Fabricated by a Seed-Mediated Growth Approach. *The Journal of Physical Chemistry B* 109(3): 1204-1209.
- Chen, J., Wiley, B., McLellan, J., Xiong, Y., Li, Z. & Xia, Y. 2005. Optical Properties of Pd–Ag and Pt–Ag Nanoboxes Synthesized via Galvanic Replacement Reactions. *Nano Letters* 5(10): 2058-2062.
- Chen, S., Wang, Z. L., Ballato, J., Foulger, S.H. & Carrol, D.L. 2003. Monopod, Bipod, Tripod, and Tetrapod Gold Nanocrystals. *Journal of The American Chemical Society* 125(52): 16186-16187.
- Gou, L. & Murphy, C.J. 2003. Solution-Phase Synthesis of  $\text{Cu}_2\text{O}$  Nanocubes. *Nano Letters* 3(2): 231-234.
- Hao, E., Bailey, R.C., Schatz, G.C., Hupp, J.T. & Li, S. 2004. Synthesis and Optical Properties of “Branched” Gold Nanocrystals. *Nano Letters* 4(2): 327-330.
- Im, S.H., Lee, Y.T., Wiley, B. & Xia, Y. 2005. Large-Scale Synthesis of Silver Nanocubes: The Role of HCl in Promoting Cube Perfection and Monodispersity. *Angewandte Chemie International Edition* 44(14): 2154-2157.
- Kambayashi, M., Zhang, J. & Oyama M. 2005. Crystal Growth of Gold Nanoparticles on Indium Tin Oxides in the Absence and Presence of 3-Mercaptopropyl-trimethoxysilane. *Crystal Growth & Design* 5(1): 81-84.
- Kuo, C. & Huang, M.H. 2005. Synthesis of Branched Gold Nanocrystals by a Seeding Growth Approach. *Langmuir* 21(5): 2012-2016.
- Lin, Z., Cai, J.J., Scriven L.E. & Davis, H.T. 1994. Spherical-to-Wormlike Micelle Transition in CTAB Solutions. *The Journal of Physical Chemistry* 98(23): 5984-5993.
- Murphy, C.J., Sau, T.K., Gole, A.M., Orendorff, C.J., Gao, J., Gou, L., Hunyadi, S.E. & Li, T. 2005. Anisotropic Metal Nanoparticles: Synthesis, Assembly, and Optical Applications. *The Journal of Physical Chemistry B* 109(29): 13857-13870.
- Oyama, M. 2010. Recent Nanoarchitectures in Metal Nanoparticle-modified Electrodes for Electroanalysis. *Analytical Sciences* 26(1): 1-12.
- Oyama, M., Ali Umar, A. & Zhang, J. 2010. Recent Advances in Metal Nanoparticle-Attached Electrodes. *Advanced Nanomaterials, Vol. 1* (K. E. Geckeler and H. Nishide, Eds.). Wiley-VCH. P. 297-318.

- Sun, Y. & Xia, Y. 2002. Shape-Controlled Synthesis of Gold and Silver Nanoparticles. *Science* 298: 2176-2179.
- Törnblom, M. & Henriksson, U. 1997. Effect of Solubilization of Aliphatic Hydrocarbons on Size and Shape of Rodlike C<sub>16</sub>TABr Micelles Studied by <sup>2</sup>H NMR Relaxation. *The Journal of Physical Chemistry B* 101(31): 6028-6035.
- Tsuji, M., Hashimoto, M., Nishizawa, Y., Kubokawa, M. & Tsuji, T. 2005. Microwave-Assisted Synthesis of Metallic Nanostructures in Solution. *Chemistry – A European Journal* 11(2): 440-452.
- Wiley, B., Sun, Y., Mayers, B. & Xia, Y. 2005. Shape-Controlled Synthesis of Metal Nanostructures: The Case of Silver. *Chemistry – A European Journal* 11(2): 454-463.
- Wu, H., Liu, M. & Huang, M.H. 2006. Direct Synthesis of Branched Gold Nanocrystals and Their Transformation into Spherical Nanoparticles. *The Journal of Physical Chemistry B* 110(39): 19291-19294.
- Xiong, Y., Chen, J., Wiley, B., Xia, Y., Aloni, S. & Yin, Y. 2005a. Understanding the Role of Oxidative Etching in the Polyol Synthesis of Pd Nanoparticles with Uniform Shape and Size. *Journal of The American Chemical Society* 127(20): 7332-7333.
- Xiong, Y., McLellan, J.M., Chen, J., Yin, Y., Li, Z. & Xia, Y. 2005b. Kinetically Controlled Synthesis of Triangular and Hexagonal Nanoplates of Palladium and Their SPR/SERS Properties. *Journal of The American Chemical Society* 127(48): 17118-17127.
- Xiong, Y., Wiley, B., Chen, J., Xia, Y., Yin, Y. & Li, Z. 2005c. Size-Dependence of Surface Plasmon Resonance and Oxidation for Pd Nanocubes Synthesized via a Seed Etching Process. *Nano Letters* 5(7): 1237-1242.
- Yu, D. & Yam, V.W. 2004. Controlled Synthesis of Monodisperse Silver Nanocubes in Water. *Journal of The American Chemical Society* 126(41): 13200-13201.

Munetaka Oyama\*  
Department of Material Chemistry  
Graduate School of Engineering  
Kyoto University  
Nishikyo-ku, Kyoto 615-8520  
Japan

Akrajias Ali Umar, Muhamad Mat Salleh  
& Burhanuddin Yeop Majlis  
Institute of Microengineering and Nanoelectronics  
Universiti Kebangsaan Malaysia  
43600 UKM Bangi, Selangor  
Malaysia

\*Corresponding author; email: oyama.munetaka.4m@kyoto-u.ac.jp

Received: 10 December 2010

Accepted: 20 January 2011